Research on Engineering Structures & Materials
www.jresm.org
Research Group

Research Article

Experimental investigation of composite hollow steel-concrete double corbels

Ruqaya Saeed Mankhi [*,a], Nasser Hakeem Tu'ma [b]

Civil Engineering Department, University of Misan, Misan, Iraq

Article Info

Article History:

Received 10 Aug 2026

Accepted 17 Sep 2026

Keywords:

Double corbel;
Structural behavior;
Composite steel-concrete;
Hollow steel section

Abstract

Five corbels composed of reinforced concrete were tested for this investigation with identical dimensions and a constant concrete compressive strength of 30 MPa. The specimens were tested under monotonic loading using a single-point loading system. One specimen was used as a control specimen without strengthening, designated as (D-C-F30-0.2). Hollow steel sections (HSS) with various strengthening configurations and shear span-to-depth ratios were used to reinforce the remaining four specimens. The first strengthened specimen, designated as (D-P-SS-F30-0.2), was reinforced in the horizontal and inclined strut regions using hollow steel sections to enhance the compressive force-transfer mechanism within the corbel. The second specimen, designated as (D-P-TSS-F30-0.2), was strengthened in the horizontal and inclined strut regions in addition to the tie region at a ratio of 0.2. The third specimen, designed as D-P-TSS-F30-0.3, employed the same strengthening configuration with a ratio of 0.3 to examine the impact of increasing the shear span-to-depth ratio on the structural response. Similarly, the fourth specimen, designated as (D-P-TSS-F30-0.35), was strengthened in the horizontal and inclined strut regions together with the tie region, with a ratio of 0.35. The experimental program was designed to evaluate the influence of the strengthening configuration and the variation in the ratio on the structural behavior of reinforced concrete corbels in terms of crack propagation, stiffness, load-carrying capacity, toughness, ductility, and failure mechanism.

© 2026 MIM Research Group. All rights reserved.

1. Introduction

In reinforced concrete (RC), corbels are short cantilevers that extend from walls or columns and have a low a/d ratio. ACI 318-19 [1] limits the value of the a/d ratio (shear span / effective depth) for corbels to less than 2; however, Mattock et al. [2] classified cantilevers possessing an a/d ratio not exceeding one as corbels. Corbels are designed to withstand enormous loads from cranes in heavy-duty manufacturing workshops, precast buildings, and bridges, as well as horizontal forces generated by temperature changes, creep, or restricted shrinkage [3–5]. The RC corbel element is primarily controlled by shear rather than moment and experiences a high concentration of tensile stress, known as a disturbed region. Consequently, the strut-tie model is often used to analyze the mechanism of corbel strength, with tensioned regions modeled as tie reinforcement and the compressive zone modeled as a concrete strut. Corbels possessing an a/d ratio of less than one has been studied using shear friction. The failure path is the route where structural elements dissipate the least energy. Causes of failure include shearing, tension tie yielding, compression strut splitting or crushing, and shearing failure beneath a loading plate or localized bearing [6, 7].

In certain instances, such as alterations in usage, design flaws, or degradation from inclement weather, the corbel needs reinforcement or enhancement [8]. Earlier research on corbel

*Corresponding author: st_chem20242@uomisan.edu.iq
[a]orcid.org/0009-0006-4632-1565; [b]orcid.org/0000-0003-1956-8539
DOI: http://dx.doi.org/10.17515/resm2026-2149ic0810rs

strengthening employed three main approaches: post-tensioned anchored bars, external strengthening with steel plates, and exterior reinforcement with FRP composites [8, 9]. Heidayet et al. [10] found that after fixing multiple damaged RC corbels with external plates, the repaired corbels' strength ratio varied between 0.7 and 1.5. El-Maaddawy and El-Sayed [11] found that CFRP sheets provided a strength gain of between 21% and 40%. Mohammed and Hassan [12] discovered that assessing CFRP-wrapped high-strength concrete corbels enhanced their load capacity by 28.3%. Ivanova and Assih [13] investigated the use of carbon fiber textiles to strengthen RCCs, achieving a failure tensile strength of over 1.82. They also evaluated the static and dynamic response of RCC reinforced with carbon fibers; stiffness increased by less than one-third, but the ultimate load doubled [14]. Urban and Krawczyk [15] proposed using post-installed threaded rods for additional support. Mohammad and AlShamaa [16] studied how Near Surface Mounted (NSM) CFRP strips enhance the condition of reacting powder concrete brackets, achieving an average gain of 15%.

Al-Kamaki et al. [17] used CFRP textiles to analyze the behavior of externally reinforced RCCs, finding that diagonal reinforcement increased final strength by 27%. The experimental reaction of high-strength self-consolidating reinforced concrete (RCC) with near-surface-mounted (NSM) steel bars was evaluated by Shakir and Kamonna [18]. They investigated four different configurations for placing reinforcing bars. For a/d ratios of 0.85 and 1.25, the maximum enhancements in failure load were 57% and 41%, respectively. Braidi et al. [19] examined the performance of hollow steel-concrete composite columns exposed to unconventional tensile pressures via an experimental program comprising seven laboratory specimens. The findings indicated that incorporating a hollow steel segment within the column enhanced the tensile strength by as much as 17% relative to traditional columns. The research indicated that maximum tensile resistance was attained when the loading eccentricity approached the balanced eccentricity (±15%). Despite the extensive investigation of RC corbel strengthening using external steel plates, FRP systems, NSM reinforcement, and post-installed steel bars, the use of embedded hollow steel sections (HSS) as an internal strengthening component for RC corbels has received limited experimental attention. The proposed technique differs from conventional steel-based, externally bonded, and steel–concrete composite strengthening systems by embedding HSS within the concrete body and strategically positioning them within the principal strut and tie regions identified by the strut-and-tie model (STM). Thus, rather than relying primarily on external reinforcement or surface-bonded strengthening, the proposed system integrates the HSS directly into the internal load-transfer mechanism of the corbel. This configuration is intended to enhance the load-transfer capacity of the principal strut and tie regions while maintaining the integrity of the external concrete surfaces. The present study experimentally evaluates the structural response of RC corbels strengthened using different HSS configurations under monotonic loading, with emphasis on load-carrying capacity, deformation, stiffness, toughness, crack propagation, and failure modes.

2. Experimental Work

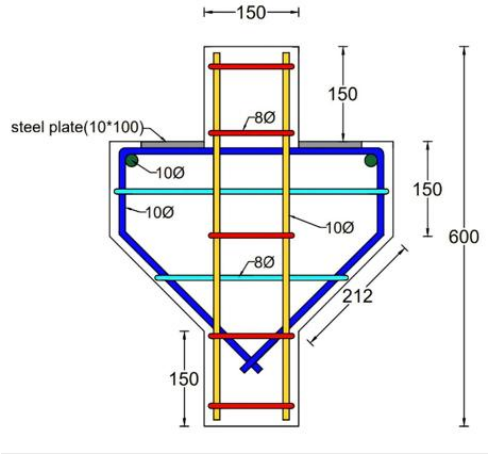
2.1 Specimen Description

Five reinforced concrete corbels were tested for this investigation with identical dimensions and a constant concrete compressive strength of 30 MPa, see Figure 1. The specimens were tested under monotonic loading using a single-point loading system. One specimen was used as a control specimen without strengthening, designated as D-C-F30-0.2, with an a/d ratio equal to 0.2. Hollow steel sections (HSS) with various strengthening configurations and shear span-to-depth ratios were used to reinforce the remaining four specimens. The first strengthened specimen, designated as (D-P-SS-F30-0.2), was reinforced in the horizontal and inclined strut regions using hollow steel sections to enhance the compressive force-transfer mechanism within the corbel. The second specimen, designated as (D-P-TSS-F30-0.2), was strengthened in the horizontal and inclined strut regions in addition to the tie region at a ratio of 0.2. The third specimen, designed as D-P-TSS-F30-0.3, employed the same strengthening configuration with a ratio of 0.3 to explore the influence of raising the shear span-to-depth ratio on the structural response. Similarly, the fourth specimen, designated as (D-P-TSS-F30-0.35), was strengthened in the horizontal and inclined strut regions together with the tie region, with a ratio of 0.35. The experimental program was designed to

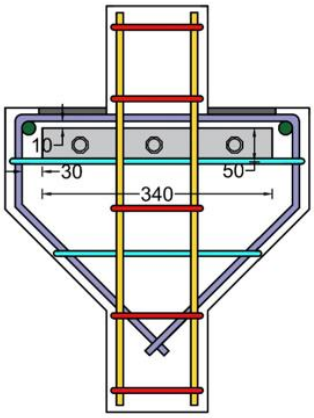
evaluate the influence of the strengthening configuration and the variation in the ratio on the structural behavior of reinforced concrete corbels in terms of crack propagation, stiffness, load-carrying capacity, toughness, ductility, and failure mechanism.

2.2 Materials

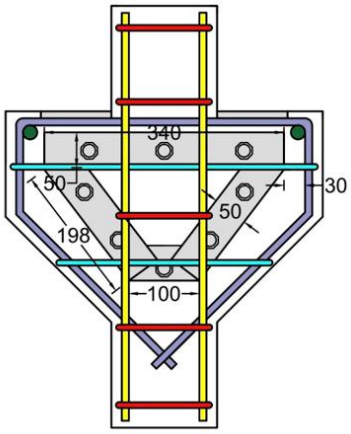
This investigation utilized ordinary Portland cement (Crista) in accordance with IQS No. 5/2019 [20]. Natural sand from the Basra Governorate, with a maximum particle size of 4.75 mm, was utilized as fine aggregate, and crushed gravel with a maximum size of 10 mm was employed as coarse aggregate. Both aggregates satisfied the specifications of IQS45/1984 [21]. The sieve analysis results are presented in Tables 1 and 2.



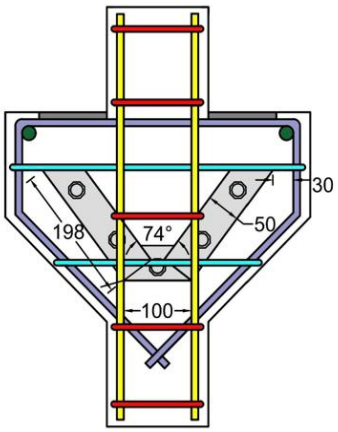
D-C-F30-0.2



D-P-T-F30-0.2



D-P-TSS-F30-0.2, D-P-TSS-F30-0.3, D-P-TSS-F30-0.35



D-P-SS-F30-0.2

Fig. 1. Details of the reinforcement and geometry of the tested corbel

Table 1. Fine aggregate (sand) grading

No	Sieve size (mm)	Percent passing (%)	Iraqi Specification IQS45/1984 for Zone (2)
1	10	100	100
2	4.75	97.8	90-100
3	2.36	88.8	75-100
4	1.18	75.4	55-90
5	0.6	57	35-59
6	0.3	26.6	8-30
7	0.15	3.4	0-10
Materials passing through a sieve 75 micron (%)		4.2	≤ 5%

Table 2. Coarse aggregate grading

No.	Sieve size (mm)	Percent passing (%)	Iraqi Specification IQS45/1984 for Zone (2)
1	12.5	100	100
2	9.5	100	85-100
3	4.75	10	25-0
4	2.36	1	5-0

In compliance with Iraqi standards, reverse osmosis (RO) water was utilized to mix and cure the concrete samples, specification (IQS 1703/2018) [22]. Steel reinforcing bars with deformations of Ø10 mm and Ø8 mm were used. Several steel hollow boxes of varying sizes were employed. The square hollow box has two alternative dimensions (50×50 mm). The materials complied with ASTM A615/A615M-20 [23] for reinforcement bars and ASTM A370-10 [24] for steel section evaluation. Table 3 presents the characteristics of the reinforcing bars and steel sections. Since the geometry of the tested corbels required non-standard steel configurations, the hollow steel sections (HSS) were fabricated from separate steel pieces that were cut to the required dimensions and subsequently assembled using electric arc welding. The welding electrodes used were J38.12/E6013, with a diameter of 2.5 mm. According to the American Welding Society Standard (AWS D1.1/D1.1M:2020) [25], these electrodes can be used with AC or DC polarity, with a recommended welding current of 50–90 A. The assembled steel components were connected using fillet welds with a nominal weld size of 3 mm, in accordance with ANSI/AISC 360-22 [26]. After welding, the connections were visually inspected to check the general appearance and continuity of the welds and to identify any visible surface defects. Steel bearing plates (150 × 100 × 10 mm) were welded to the primary tension reinforcement. Steel bolts were used as shear connectors between the hollow steel sections (HSS) and the surrounding concrete. The bolts had a diameter of 9 mm and a total length of 50 mm. The bolts were welded directly to the HSS before concrete casting using electric arc welding. The shear connectors were spaced at 15 cm along the member.

Table 3. Average characteristics of steel sections and reinforcing bars

$D_{nominal}$(mm)	Test results	
	Yield strength (N/mm²)	Ultimate strength (N/mm²)
10mm	650	807
8mm	338	563
Hollow steel box (50×50)	320	375

2.3 Concrete Mix Design

In this study, normal concrete with different compressive strengths was used, based on the mix proportions presented in Table 4.

Table 4. Concrete mix percentages

No.	Materials	30 (kg/m^3)
1	Cement	412
2	Water	212
3	Gravel	1064
4	Sand	656

2.4 Fresh Concrete Tests

To check the quality of the concrete mix while casting the major specimens, the workability of the concrete mixes was evaluated using the slump test according to ASTM C143 [27]. The results of the slump test are summarized in Table 5.

Table 5. Slump test results

No.	Type of concrete	Slump value (mm)
1	f_c30	100

2.5 Mechanical Properties of Hardened Concrete

The tests on hardened concrete were performed in the laboratory. Three cylinders with a measurement of 100x200 mm were tested in compliance with ASTM C31/C31M-21 to ascertain the concrete's compressive strength [28]. Three prisms with a measurement of 100x100x500 mm were used to determine flexural strength in accordance with ASTM C78-02 [29]. Three cylinders measuring 100×200 mm were utilized for the splitting tensile strength test in compliance with ASTM C496-17 [30]. Table 6 presents the findings of the tests conducted.

Table 6. Summary of test results on hardened concrete

Compressive strength f_{cu} (MPa)	Flexural strength (MPa)	Tensile strength f_t (MPa)
29	3.3	2.9

2.6 Test Setup and Instrumentation

Figure 2 shows the equipment test that had a 1000 kN load capacity, which was utilized to test each sample. The machine can regulate and modify the loading rate as necessary. A linear variable differential transformer (LVDT) was positioned beneath the corbel during the loading process to quantify deflection.



Fig. 2. Testing devices, LVDT, and data logger

3. Results and Discussion

The tested specimens, along with the cracking load, maximum load, maximum deflection, and mode of failure, are displayed in Table 7. A thorough description of each specimen may be found below.

Table 7. Experimental test results of specimens

Specimen	Load (kN)		Max deflection, mm	Mode of failure
	Cracking, Pcr	Ultimate, Pu		
D-C-F30-0.2	100	250	3.5	Shear compression failure
D-P-SS-F30-0.2	250	400	3.7	Shear tension failure
D-P-TSS-F30-0.2	230	538.5	2.5	Shear tension failure
D-P-TSS-F30-0.3	250	692.5	2.6	Shear tension failure
D-P-TSS-F30-0.35	240	500	3.1	Shear tension failure

3.1 Mode of Failure and Crack Propagation of Specimens

Figure 3 illustrates the crack propagation patterns and failure modes of the tested reinforced concrete corbels, highlighting the impact of the a/d ratio and strengthening configuration on the structural response in the context of the strut-and-tie mechanism. The control specimen (D-C-F30-0.2) exhibited the initial crack at roughly 100 kN, initiating from the loading region and propagating toward the column face. Failure occurred in shear compression accompanied by crushing in the nodal zone at an ultimate load of approximately 250 kN. This is early cracking. Subsequent failures are likely due to the lack of internal reinforcement, leading to rapid stress concentration in the concrete. Specimen (D-P-SS-F30-0.2) which exhibited the first crack at approximately 250 kN, initiating from the loading region and propagating toward the corbels-column interface. The specimen reached an ultimate load of approximately 400 kN, representing an increase of about 60% compared with the control specimen, before failure occurred in shear tension. The delayed crack initiation suggests that the hollow steel section effectively redistributed internal stresses.



D-C-F30-0.2 D-P-SS-F30-0.2 D-P-TSS-F30-0.35

D-P-TSS-F30-0.2 D-P-TSS-F30-0.3

Fig. 3. Mode of failure of the corbels. Scale = 1:10.5; scale bar = 100 mm

In specimen (D-P-TSS-F30-0.2), the first crack appeared at approximately 230 kN, initiating from the loading region and propagating toward the column face. The specimen achieved an ultimate load of approximately 538.5 kN, corresponding to an increase of about 115% relative to the control specimen. This enhanced performance could be attributed to the dual action of the steel section in both tension and compression zones, which strengthened the internal truss mechanism. Specimen (D-P-TSS-F30-0.3) demonstrated the best structural performance. The first crack appeared at approximately 250 kN, initiating from the load region and propagating toward the column face. The specimen reached an ultimate load of approximately 692.5 kN, indicating a rise of almost 177% in comparison to the control specimen. It is hypothesized that the a/d ratio of 0.3 provides an optimal

balance, allowing for a more efficient load transfer path away from the critical column face. In contrast, specimen (D-P-TSS-F30-0.35) exhibited the first crack at approximately 240 kN, propagating from the loading region toward the corbel face, while failure occurred in shear tension failure at an ultimate load of approximately 500 kN. The relative decrease in capacity might be linked to the increased shear span, which potentially enhanced the bending effect and accelerated the shear tension failure. Overall, all strengthened specimens exhibited delayed crack initiation, redirected crack paths, and improved load-carrying capacity. These findings indicate the effectiveness of the strengthening systems in enhancing internal stress transfer within the critical region of the corbels.

3.2 Load-Deflection Curve

The load-deflection curves of the tested reinforced concrete corbels (Figure 4) showed clear differences in stiffness, load-carrying capacity, and deformation behavior depending on the strengthening configuration and a/d ratio. The control specimen (D-C-F30-0.2) exhibited the lowest structural performance, reaching an ultimate load of about 250 kN with a deflection of 3.5 mm, attributed to limited crack resistance and poor stress redistribution due to the absence of strengthening. Specimen (D-P-SS-F30-0.2) showed improved behavior, reaching an ultimate load of about 400 kN with a deflection of 3.7 mm, indicating better load transfer and partial crack control. Specimen (D-P-TSS-F30-0.2) achieved higher performance, reaching about 538.5 KN with a lower deflection of 2.5 mm, reflecting a more efficient strut-and-tie mechanism and improved stress distribution. The best performance was recorded in specimen (D-P-TSS-F30-0.3), which reached an ultimate load of about 692.5 kN with a deflection of 2.6 mm, suggesting an optimal load path and enhanced corbel action. In contrast, specimen (D-P-TSS-F30-0.35) showed lower performance, reaching about 500 kN with a deflection of 3 mm, due to reduced load transfer efficiency at a higher a/d ratio. Overall, the strengthened specimens demonstrated improved stiffness and load-carrying capacity compared with the control specimen, while an a/d ratio of 0.3 provided the most balanced structural response.

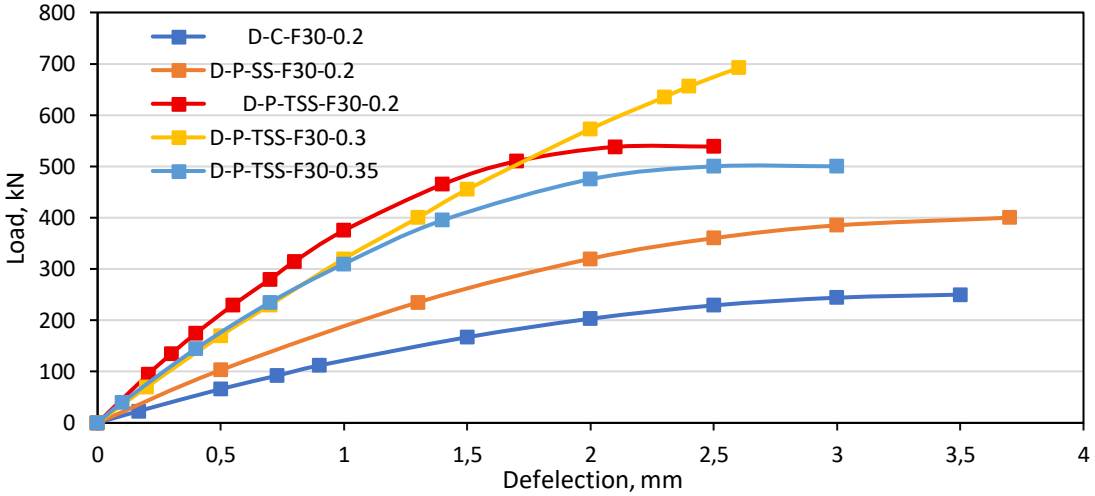


Fig. 4. Load-deflection curves for all examined specimens

3.3 Stiffness, Toughness, and Ductility

Stiffness (K) measures the resistance to deformation exhibited by an elastic body. The effective secant stiffness, which corresponds to the load stage (0.75Pu), is used for evaluation [31], as represented by Eq. (1).

$$K_{eff} = \frac{0.75_{Pu}}{\Delta_{0.75pu}} \quad (1)$$

Where; K_{eff} : effective stiffness, Pu: ultimate load, $\Delta_{0.75pu}$: deflection value corresponding to the 0.75 Pu load level.

The control specimen (D-C-F30-0.2) recorded the lowest stiffness value of 104.16 kN/mm, while all strengthened specimens showed noticeable improvement. Specimen (D-P-SS-F30-0.2) revealed a rise in stiffness of around 80% in contrast to a control specimen, whereas specimen (D-P-TSS-F30-0.2) achieved the highest increase of about 189%. Similarly, specimens (D-P-TSS-F30-0.3) and (D-P-TSS-F30-0.35) showed increases of approximately 178.5% and 177%, respectively. The area under the load-deflection curve, which represents toughness, is a measure of a member's resistance to deformation before failure [32], as represented by Eq. (2).

$$T=\int_0^{\Delta u} P(\Delta)\, d\Delta \tag{2}$$

Where; T: toughness, P = load (Kn), Δ: The deflection (mm), Δu: The deflection at the ultimate load.

The control specimen recorded the lowest toughness value of 581 kN mm, while all strengthened specimens demonstrated clear improvement. Specimens (D-P-SS-F30-0.2), (D-P-TSS-F30-0.2), and (D-P-TSS-F30-0.3) exhibited a similar increase in toughness of approximately 71%, whereas specimen (D-P-TSS-F30-0.35) achieved the highest increase of about 84.5% compared with the control specimen. This behavior indicates improved stress redistribution and delayed crack propagation due to strengthening. Ductility (μ), which is represented by Eq. (3) [33], is the capacity to withstand inelastic deformation without reducing the ultimate load till failure. ductility index was calculated as the ratio of the ultimate deflection (Δ_u) to the yield deflection (Δ_y), as shown in Figure 5.

$$\mu = (\Delta_u/\Delta_y) \tag{3}$$

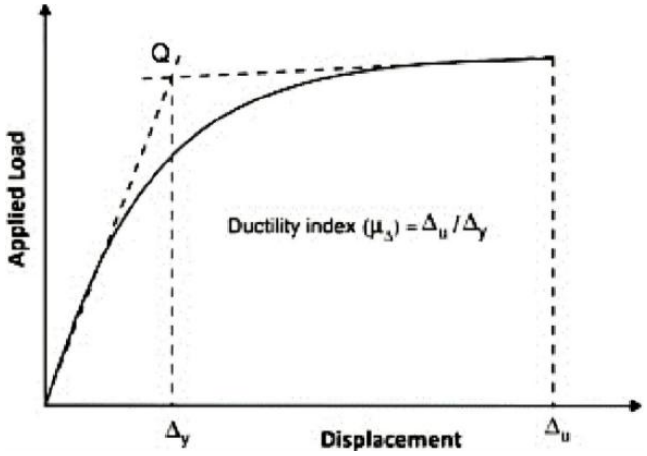


Fig. 5. Calculating the ductility ratio using the displacement ratio method

where μ is the ductility index, Δ_u is the displacement at ultimate load (mm), and Δ_y is the displacement corresponding to the service load (mm). The service displacement was determined from the intersection of the tangents to the initial and final portions of the load–deflection curve.

Table 8. Results of stiffness, toughness, and ductility for all specimens

No.	Specimens	Stiffness (kN/mm)	Toughness (kN·mm)	Ductility
1	D-C-F30-0.2	104.16	581	4.38
2	D-P-SS-F30-0.2	187.5	995	3.89
3	D-P-TSS-F30-0.2	301	1000	4.44
4	D-P-TSS-F30-0.3	290.15	994.5	4.73
5	D-P-TSS-F30-0.35	288.46	1072	5

The control specimen recorded a ductility value of 4.375. The specimen (D-P-SS-F30-0.2) showed a reduction in ductility of approximately 11%, indicating a stiffer response with lower deformation capacity. In contrast, specimen (D-P-TSS-F30-0.2) exhibited a slight increase of about 1.5%, and (D-P-TSS-F30-0.35) achieved increases of approximately 8.1% and 14.3%, as represented, see Table 8. This improvement may be attributed to enhanced stress redistribution and delayed sudden failure.

4. Conclusions

Based on the experimental investigation of reinforced concrete corbels with and without the proposed embedded hollow steel section strengthening system, the following conclusions can be drawn:

- The incorporation of hollow steel sections within the corbels resulted in a clear improvement in ultimate load capacity compared with the unstrengthened control specimen. The control specimen (D-C-F30-0.2) reached an ultimate load of approximately 250 kN, whereas the strengthened specimens reached higher capacities. The increases were approximately 60% for D-P-SS-F30-0.2, 115% for D-P-TSS-F30-0.2, 177% for D-P-TSS-F30-0.3, and 100% for D-P-TSS-F30-0.35.
- The strengthening system delayed the formation of the first visible cracks. The control specimen cracked at approximately 100 kN, while the strengthened specimens developed their first visible cracks at loads ranging from approximately 230 to 250 kN. This indicates improved resistance to crack initiation under the applied monotonic loading. The strengthening configuration affected the stiffness and deformation response of the corbels. The effective secant stiffness increased substantially in the strengthened specimens relative to the control specimen. The increases were approximately 80% for D-P-SS-F30-0.2, 189% for D-P-TSS-F30-0.2, 178.5% for D-P-TSS-F30-0.3, and 177% for D-P-TSS-F30-0.35.
- The load–deflection responses demonstrated that the strengthened specimens generally sustained higher loads with comparable or lower deflections than the control specimen. In particular, D-P-TSS-F30-0.3 achieved the highest ultimate load of approximately 692.5 kN at a deflection of approximately 2.6 mm, indicating the highest load-carrying capacity among the tested configurations.
- The toughness of the strengthened specimens was higher than that of the control specimen. The control specimen recorded a toughness of 581 kN·mm, whereas the strengthened specimens showed increases ranging from approximately 71% to 84.5%. The highest increase was obtained for D-P-TSS-F30-0.35.
- The measured ductility indices showed that strengthening did not produce a uniform increase in deformation capacity. D-P-SS-F30-0.2 exhibited a reduction in ductility, whereas D-P-TSS-F30-0.2 and D-P-TSS-F30-0.35 showed higher ductility indices than the control specimen. Therefore, the effect of strengthening on ductility depended on the strengthening configuration and a/d ratio.
- The observed crack patterns and failure modes indicate that the strengthened specimens developed cracks at higher load levels and exhibited changes in crack propagation compared with the control specimen. The control specimen failed by shear compression, whereas the strengthened specimens primarily exhibited shear-related failure modes.
- Among the investigated configurations, D-P-TSS-F30-0.3 provided the highest ultimate load and a relatively low ultimate deflection. Within the tested range, the a/d ratio of 0.3 therefore produced the highest measured load-carrying capacity for the combined strut-and-tie strengthening configuration.
- Overall, the experimental results demonstrate that the proposed hollow steel section strengthening system can substantially improve the load-carrying capacity, stiffness, and toughness of the tested reinforced concrete corbels. The magnitude of improvement was dependent on the strengthening configuration and a/d ratio.

References

[1] American Concrete Institute. 318-19 Building code requirements for structural concrete and commentary. American Concrete Institute; 2019.

[2] Mattock AH, Chen KC, Soongswang K. The behavior of reinforced concrete corbels. PCI Journal. 1976;21(2):52-77. https://doi.org/10.15554/pcij.03011976.52.77

[3] Shakir QM. Performance assessment of high-strength concrete two-sided corbels with embedded stiffened web-rolled steel. Structures. 2021;32:1469-1480. https://doi.org/10.1016/j.istruc.2021.03.098

[4] Shakir QM, Abdlsaheb SD. Rehabilitation of partially damaged high-strength RC corbels by EB FRP composites and NSM steel bars. Structures. 2022;38:652-671. https://doi.org/10.1016/j.istruc.2022.02.023
[5] Torres FM. Theoretic-experimental analysis of reinforced concrete corbels [Master's thesis]. São Paulo: São Paulo University; 1998.
[6] Shakir QM. Behavior of high-performance RC composite corbels with inclined stirrups. Canadian Journal of Civil Engineering. 2022;49:18-30. https://doi.org/10.1139/cjce-2020-0149
[7] Shakir QM, Abdlsaheb SD. Strengthening of the self-compacted reinforced concrete corbels using NSM steel bars and CFRP sheets techniques. Journal of Engineering Science and Technology. 2022;17(3):1764-1780.
[8] Neupane RC, Eddy L, Nagai K. Investigation on strengthening approaches adopted for poorly detailed RC corbels. Fibers. 2017;5(2):16. https://doi.org/10.3390/fib5020016
[9] de Souza RA, Trautwein LM, Ferreira M de P. Reinforced concrete corbel strengthened using carbon fiber reinforced polymer (CFRP) sheets. Journal of Composites Science. 2019;3(1):26. https://doi.org/10.3390/jcs3010026
[10] Heidayet A, Ramadhan A, Qarani O. Repairing of damaged reinforced concrete corbels strengthened by externally bonded steel plates. Zanco Journal of Pure and Applied Sciences. 2004;16(1).
[11] El-Maaddawy TA, Sherif E-SI. Response of concrete corbels reinforced with internal steel rebars and external composite sheets: Experimental testing and finite element modeling. Journal of Composites for Construction. 2014;18(2). https://doi.org/10.1061/(ASCE)CC.1943-5614.0000403
[12] Mohammed AA, Hassan GB. Load capacity and deformation of high-strength concrete corbels wrapped with CFRP sheets. In: The 2nd International Conference of Buildings, Construction and Environmental Engineering (BCEE2-2015); 2015.
[13] Ivanova I, Assih J. Experimental study of local behavior of strengthened reinforced concrete short corbel by bonding carbon fiber fabrics. International Journal of Structural and Civil Engineering Research. 2015.
[14] Ivanova I, Assih J. Static and dynamic experimental study of a strengthened reinforced short concrete corbel using carbon fabrics, crack path in the shear zone. Frattura ed Integrità Strutturale. 2015;34:90-98. https://doi.org/10.3221/IGF-ESIS.34.09
[15] Urban T, Krawczyk Ł, Gołdyn M. Strengthening of short reinforcement concrete corbel using steel accessory.
[16] Mohammad AKQ, Al-Shamaa MFK. Experimental study of behaviour of reactive powder concrete strengthening by NSM-CFRP corbels. Civil Engineering Journal. 2018;4:980-992. https://doi.org/10.28991/cej-0309150
[17] Al-Kamaki YSS, Hassan GB, Alsofi G. Experimental study of the behaviour of RC corbels strengthened with CFRP sheets. Case Studies in Construction Materials. 2018;9:e00181. https://doi.org/10.1016/j.cscm.2018.e00181
[18] Shakir QM, Kamonna HHH. The behavior of high-strength self-compacting reinforced concrete corbels strengthened with NSM steel bars. International Journal of Advanced Science, Engineering and Information Technology. 2018;8:1022-1028. https://doi.org/10.18517/ijaseit.8.4.5905
[19] Braidi WI, Mohsin RD, Tu'ma NH, Raheem HAK. Experimental investigation of eccentric composite hollow steel-concrete tensioned column. Civil and Environmental Engineering. 2026. https://doi.org/10.2478/cee-2026-0061
[20] Central Organization for Standardization and Quality Control. Iraqi specifications 5/2019: Portland Cement. Iraq; 2019.
[21] Central Organization for Standardization and Quality Control. Iraqi Specification No. 45: Natural sources for gravel that is used in concrete and construction. Baghdad, Iraq; 1984.
[22] Central Organization for Standardization and Quality Control. Iraqi specifications 1703/2018: Water used for concrete. Iraq; 2018.
[23] ASTM International. Standard specification for deformed and plain carbon-steel bars for concrete reinforcement (ASTM A615/A615M-20). 2020.
[24] ASTM International. Standard test method and definition for mechanical testing of steel products (ASTM A370-05). Annual Book of ASTM Standards, Vol. 01.01. Philadelphia, PA: ASTM; 2010.
[25] American Welding Society. Structural welding code-Steel. 2020.
[26] American Institute of Steel Construction (AISC). Specification for Structural Steel Buildings (ANSI/AISC 360-22). Chicago, IL: AISC; 2022.
[27] ASTM International. Standard test method for slump of hydraulic-cement concrete (ASTM C143-17). 2017.
[28] ASTM International. Standard practice for making and curing concrete test specimens in the field (ASTM C31/C31M-21a). 2021.
[29] ASTM International. Standard test method for flexural strength of concrete (using a simple beam with third-point loading) (ASTM C78-09). 2009.

[30] ASTM International. Standard test method for splitting tensile strength of cylindrical concrete specimens (ASTM C496/C496M-17). 2017.
[31] Park R. Ductility evaluation from laboratory and analytical testing. In: Proceedings of the 9th World Conference on Earthquake Engineering; 1988; Tokyo-Kyoto, Japan. p. 605-616.
[32] Shakir QM, Abd BB. Retrofitting of self-compacting RC half joints with internal deficiencies by CFRP fabrics. Jurnal Teknologi (Sciences and Engineering). 2020;82(6):49-62. https://doi.org/10.11113/jurnalteknologi.v82.14416
[33] Naaman A, Jeong M. Structural ductility of concrete beams prestressed with FRP tendons. In: Non-Metallic (FRP) Reinforcement for Concrete Structures: Proceedings of the Second International RILEM Symposium. Boca Raton, FL, USA: CRC Press; 1995. p. 379.